JOURNAL OF SOLID STATE CHEMISTRY **132,** 17–23 (1997)
ARTICLE NO. SC977385

Thermoanalytical Study, Phase Transitions, and Dimensional Changes of α-$Zr(HPO_4)_2 \cdot H_2O$ Large Crystals

Umberto Costantino,*,[1] Riccardo Vivani,* Vitezslav Zima,† and Eva Cernoskova†

** Dipartimento di Chimica, via Elce di Sotto, 8-06123 Perugia, Italy; and † Joint Laboratory of Solid State Chemistry, University of Pardubice, 530 09 Pardubice, Czech Republic*

Received September 20, 1996; in revised form February 26, 1997; accepted March 11, 1997

Crystals of millimetric dimensions of layered α-$Zr(HPO_4)_2 \cdot H_2O$ start to lose hydration water at temperatures higher than 270°C when heated at rates of 2–50°C/min. This allowed the observation, at about 143 and 257°C, of two new reversible phase transitions of monohydrate zirconium phosphate. The connected enthalpic effects were 3.8 ± 0.2 and 2.7 ± 0.1 kJ/mol, respectively. Measurements of the thickness of the crystal, along the perpendicular to the layers, were also performed as a function of the temperature. At temperatures very close to those of the two-phase transitions, the thickness of the crystal decreased by 0.69% and by a further 0.44% of its initial value. A thermal behavior very similar to that found for large crystals was observed when microcrystalline α-$Zr(HPO_4)_2 \cdot H_2O$ (average crystal size 1–10 μm) was analyzed at very high heating rates (i.e., 50°C/min). X-ray powder diffraction analysis revealed that the phase transitions involve a discontinuous decrease of the interlayer distance from 7.56 to 7.50 Å at 134°C, and to 7.43 Å at 257°C, in agreement with dilatometric data. Finally, some structural aspects involving the new phases and the possible relations with those already reported are discussed.

INTRODUCTION

Zirconium bis(monohydrogen phosphate) monohydrate, α-$Zr(HPO_4)_2 \cdot H_2O$ (hereafter referred to as α-$ZrP \cdot H_2O$), has been extensively studied in the past as a cation exchanger, an intercalating agent of polar species, and a heterogeneous catalyst; moreover it is the parent compound of a wide and emerging class of materials, the metal(IV) phosphates and phosphonates (1–3).

The crystal structure of α-ZrP was first determined in 1969 (4). Subsequent refinement (5) showed that the compound is monoclinic, with space group $P2_1/n$, cell dimensions $a = 9.060$ Å, $b = 5.297$ Å, $c = 15.414$ Å, $\beta = 101.71$ Å, $Z = 4$.

[1] To whom correspondence should be addressed.

Each layer is formed by an intermediate Zr atom plane in which each Zr atom is surrounded by a slightly distorted octahedron of oxygens belonging to six different phosphate groups. The acidic OH group of each phosphate is directed toward a neighboring layer. Owing to the stacking of the layers in the *c* direction, zeolitic cavities are formed, one per each zirconium atom. The hydration water molecules are located in these cavities. They interact with three adjacent phosphate groups, accepting two hydrogen bonds and giving a third one (6). In such a situation no hydrogen bonds are formed between the layers, which are held together only by van der Waals forces. The interlayer water is retained over phosphorus pentoxide, but it is completely lost on prolonged heating at 110°C. The loss of condensation water of monohydrogenphosphates to pyrophosphates occurs at 450–550°C.

As pointed out by several authors, the shape of the thermoanalytical (TG–DTA) curves and hence the starting and ending temperatures, as well as the extensions of thermal effects associated with the above-described transformations, are affected by external parameters, such as the heating rate, the crystallinity degree, and the particle size of the investigated sample (7–13).

However, to our knowledge, studies in the literature deal with thermal behavior of amorphous, semicrystalline, and microcrystalline samples of α-$ZrP \cdot H_2O$ by using heating rates of 10°C/min or below.

This paper describes the thermal behavior, in the 2–50°C/min heating rate range, of large crystals of α-$ZrP \cdot H_2O$ of millimetric dimensions, prepared by the method proposed by Alberti *et al.* in 1980 (14). Such behavior is quite different from that already described for microcrystalline powders, and new phase transitions of the monohydrate α-ZrP have been observed. Surprisingly, a thermal behavior very close to that found for large crystals was observed on microcrystalline samples when heated at high heating rates (>20°C/min).

0022-4596/97 $25.00

EXPERIMENTAL

Microcrystalline powder of α-$ZrP \cdot H_2O$ (average dimensions: 1–10 μm) was obtained as described in (15). Large crystals of α-$ZrP \cdot H_2O$ (0.5–2 mm of dimensions) were prepared by the slow thermal decomposition of zirconium fluorocomplexes in the presence of phosphoric acid, as reported in (14).

Coupled thermogravimetric analysis (TG) and differential thermal analysis (DTA) curves were obtained by a Stanton Redcroft STA781 thermoanalyzer at various heating rates (static atmosphere). For DTA measurements, alumina was used as the reference material.

Differential scanning calorimetry (DSC) measurements were performed by using a computer-controlled Mettler DSC 12E instrument that was previously calibrated with indium, tin, and lead standards. Samples of about 10 mg were encapsulated in aluminium sample pans and DSC curves were obtained at selected heating rates in the range 1°–20°C/min. Micrographs of the surface of the crystals before and after heating were taken by Tesla BS 340 scanning electron microscope (SEM).

The thermal changes of the thickness of the α-ZrP crystals were measured along the perpendicular to the layers in the 30–500°C temperature range. This thermomechanical analysis (TMA) was carried out with a TMA CX03R dilatometer. The analysis is based on the changes of the distance between two pistons of the sample holder with a differential capacitance displacement probe detector. The resolution of the dilatometer is about 10 nm. The force applied on the crystal was 50 mN. The heating rates used ranged from 0.1 to 50°C/min.

X-ray powder diffraction (XRD) patterns at different temperatures were obtained with an Anton Paar HTK camera mounted on a Philips PW1710 diffractometer. The patterns were collected by a step scanning procedure using a step of 0.02° 2θ and a counting time which ranged from 1 to 10 s per step, depending on the situation. The radiation used was Cu$K\alpha$, and the generator was operated at 40 kV, 30 mA.

The XRD powder patterns were indexed using the TREOR program (16).

RESULTS AND DISCUSSION

Thermal Behavior of Large Crystals of α-$ZrP \cdot H_2O$

For the sake of clarity, typical TG and DTA curves (Figs. 1a and 2a, respectively) of a sample of microcrystalline α-$ZrP \cdot H_2O$, taken at the heating rate 5°C/min, will be discussed first. The curves are in fairly good agreement with those described earlier (7, 8).

Hydration water loss starts at about 100°C. The DTA curve shows two partially overlapped endothermic effects, one sharp and the other broad, ascribed to the formation of

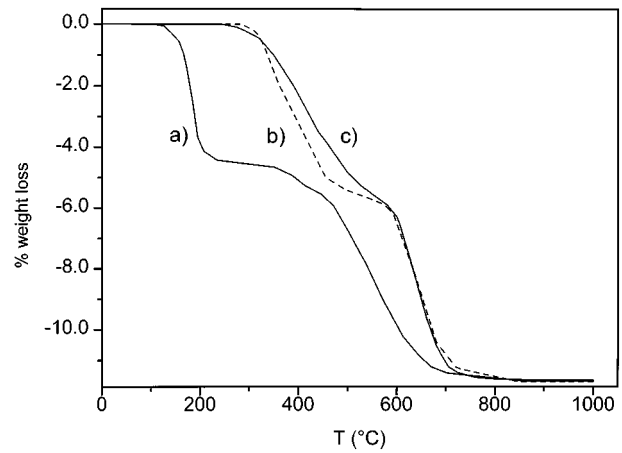

FIG. 1. TG curves of: (a) microcrystalline α-$ZrP \cdot H_2O$. Heating rate: 5°C/min; (b) large crystals of α-$ZrP \cdot H_2O$. Heating rate: 5°C/min; (c) microcrystalline α-$ZrP \cdot H_2O$. Heating rate: 50°C/min.

the anhydrous phase α-ZrP, according to the reaction

$$\alpha\text{-}ZrP \cdot H_2O(7.56) \rightarrow \alpha\text{-}ZrP(7.41) + H_2O,$$

in which the interlayer distances in angstroms are also indicated in parentheses.

A second sharp endothermic peak is then observed at about 220°C (9, 10) due to the following reversible phase transition:

$$\alpha\text{-}ZrP(7.41) \rightleftharpoons \alpha\text{-}ZrP(6.8).$$

Further heating leads to the formation of zirconium pyrophosphate with the loss of an additional mole of water per

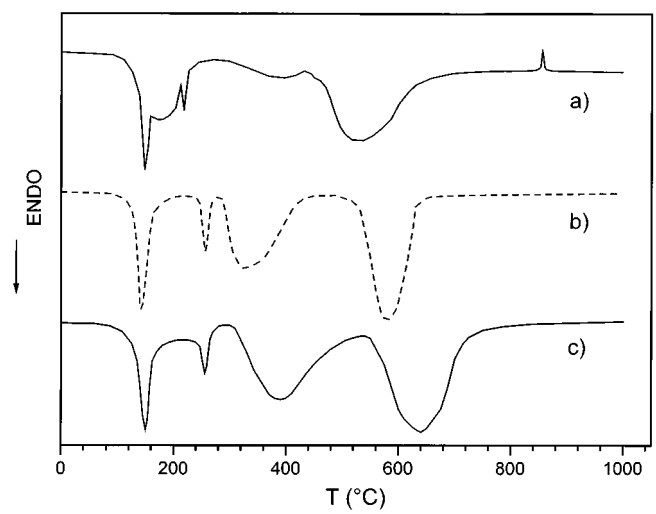

FIG. 2. DTA curves of: (a) microcrystalline α-$ZrP \cdot H_2O$. Heating rate: 5°C/min; (b) large crystals of α-$ZrP \cdot H_2O$. Heating rate: 5°C/min; (c) microcrystalline α-$ZrP \cdot H_2O$. Heating rate: 50°C/min.

mole of Zr:

$$\alpha\text{-}Zr(HPO_4)_2(6.8) \rightarrow ZrP_2O_7(6.1) + H_2O.$$

The transformation of the previously formed layered zirconium pyrophosphate (9) to the cubic one is observed as an exothermic sharp peak around 850–900°C.

TG and DTA curves obtained by heating one crystal of α-$ZrP \cdot H_2O$, of approximate dimensions $1 \times 0.8 \times 0.5$ mm and weight $\simeq 10$ mg, are shown in Figs. 1b and 2b, respectively. The heating rate was 5°C/min, the same used for the microcrystal samples.

The TG curve does not show any water loss from 20 to 270°C. On the other hand, in this range of temperatures, the DTA curve clearly shows two well-resolved endothermic effects, with a maximum at about 143 and 257°C, respectively. The two-phase transitions are reversible, as demonstrated by performing several heating and cooling cycles in the 20–270°C temperature range. Figure 3 shows the DTA profile of one heating–cooling–heating cycle as a function of the time. The two successive heatings produced almost identical endothermic effects; the corresponding exothermic effects in the cooling trace are broad and shifted at lower temperatures, probably because of kinetic effects. It seems that the reverse processes are slower than the forward ones, and the compound exhibits a significant inertia to come back to the lower temperature phases. Just after the second endothermic transition has been completed, dehydration starts and proceeds in two steps, each of which corresponds to the loss of one water molecule per formula unit, probably due to dehydration and condensation of hydrogenphosphates to pyrophosphate, respectively. At the end of the analysis the sample was ground and the XRD powder pattern was found to be that of cubic ZrP_2O_7. The experimental (11.7%) and calculated (11.96%) weight losses were in good agreement.

DSC measurements were carried out in the 25–400°C temperature range at different heating rates. In all cases the endothermic effects, already observed in the DTA curves, were well marked. Figure 4 shows a typical DSC curve obtained at a heating rate of 5°C/min. The temperatures of peak maxima are 142.5 and 254.5°C ($T_{onset} = 137.5$ and 247.2°C) respectively; the enthalpy of transitions are 3.8 ± 0.2 and 2.7 ± 0.1 kJ/mol, respectively. The shape of the TG–DTA curves seems to be independent of the heating rate. However, an unexpected phenomenon occurs at heating rates less than 2°C/min. When the crystal starts to lose water, at about 270°C, it often explodes, jumping out of the sample holder, and making the completion of the analysis rather difficult.

This effect can be explained if we suppose that dehydration occurs by diffusion of water only between the layers. In this case, the time needed for dehydration should be extremely long for crystals of such dimensions, so that even at the lowest heating rates, a very small fraction of water is lost before the temperature reaches a critical value. However, if the heating rate is very low, dehydration can occur close to the border of the crystal, allowing the formation of the anhydrous α-ZrP(7.41) phase in this region, with the result of blocking further escape of water. The pressure of water vapor at the high temperatures could then break the crystal and produce the observed explosion. Figure 5 shows SEM micrographs of the same crystal before and after thermal treatment at 300°C (heating rate: 0.2°C/min). Fracture lines, which appear on the surface of the crystal heated up to 300°C, may be due to the effect of the explosion.

Dilatometric experiments were then carried out on crystals shaped similarly to those used for TG–DTA

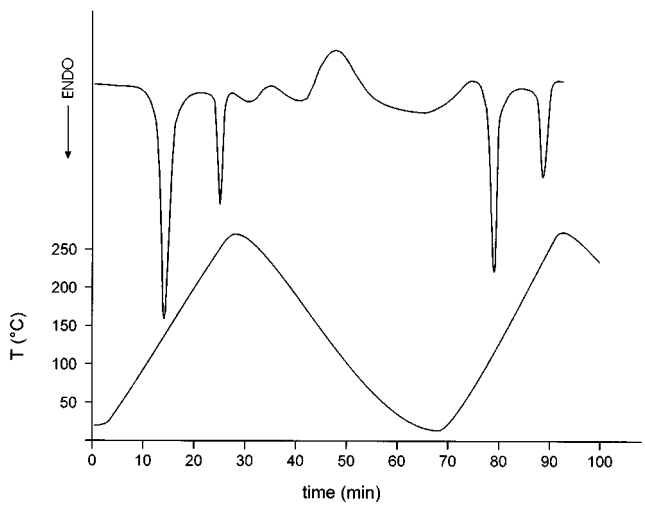

FIG. 3. DTA curve of large crystals of α-$ZrP \cdot H_2O$ as a function of the time during a heating-cooling-heating cycle. The temperature curve is reported on the bottom.

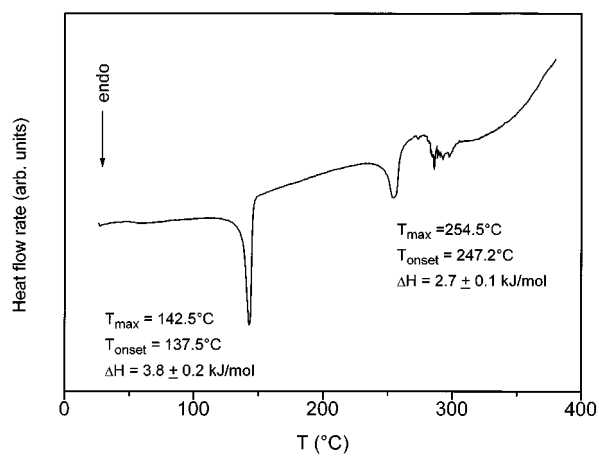

FIG. 4. DSC curve of large crystals of α-$ZrP \cdot H_2O$. Heating rate: 5°C/min.

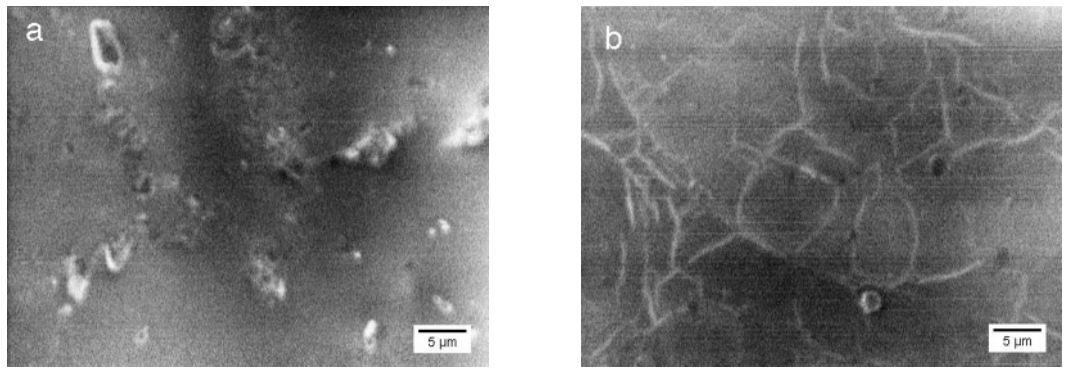

FIG. 5. SEM micrograph of a large crystal of α-$ZrP \cdot H_2O$ before (a) and after (b) heating to 300°C. Heating rate: 0.2°C/min.

experiments, and the thickness along the perpendicular to the layers was measured as a function of the temperature.

Figure 6 shows a typical TMA curve of α-$ZrP \cdot H_2O$ taken at 0.2°C/min. The expansion of the first part of the plot (Fig. 6b) shows two discontinuities: the first, occurring at about 140°C, in which the thickness is decreased by 0.69% of its initial value, and the second one, at about 250°C, with a further 0.44% decrease in thickness. Owing to this, if we assume that the interlayer distance at room temperature is 7.56 Å, we can calculate that the first phase transition involves a decrease of the interlayer distance to about 7.50 Å, and the second involves a decrease to 7.47 Å. TMA measurements also confirmed the reversibility of such phase transitions.

Just after the latter phase transition, the dilatometric plot shows a sharp increase in the thickness of the crystal, corresponding to the above-mentioned explosion, observed by TG measurements. TMA data showed that this effect disappears at heating rates higher than 10°C/min. The relatively

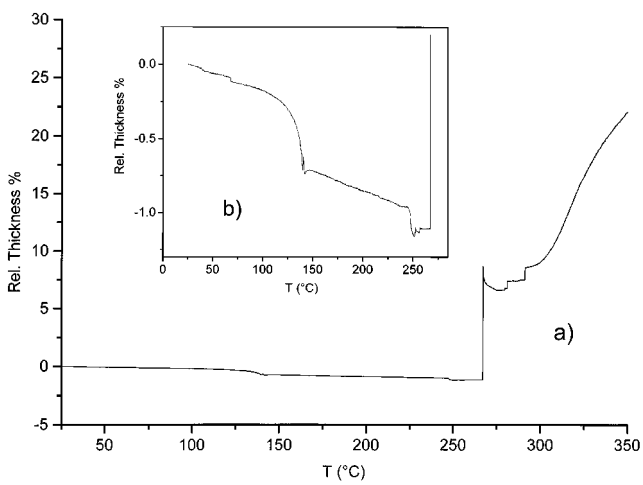

FIG. 6. TMA curve of a large crystal of α-$ZrP \cdot H_2O$ heating rate: 0.2°C/min. An expansion of the first part of the curve is shown (b).

slow increase of the crystal thickness observed above 280°C is probably caused by a further "splitting" of the layers.

Thermal Behavior of Microcrystals of α-$ZrP \cdot H_2O$ at High Heating Rates

If microcrystalline samples are heated very rapidly, hydration water loss starts at temperatures much higher than those observed for the 5°C/min heating rate ($\simeq$100°C) and it has been possible to detect the phase transitions of the hydrate phase, described above for large crystals, at heating rates as low as 20°C/min. However, the higher the heating rates are, the sharper the thermal effect becomes.

The TG and DTA curves, obtained at a heating rate of 50°C/min, of a microcrystalline sample of α-$ZrP \cdot H_2O$ are shown in Figs. 1c and 2c, respectively. Such behavior is very different from that observed for heating rates equal to or lower than 5°C/min (Figs. 1a and 2a), and, as expected, it resembles closely the behavior already discussed for large crystals (Figs. 1b and 2b). The positions of the two sharp endothermic effects (150 and 255°C) are shifted at temperatures higher than those observed for large crystals, probably due to the higher heating rate.

The first water loss starts at about 220°C. When the second phase transition has been completed, at about 260°C, the total weight loss is only 0.3%, corresponding to about 0.07 mol of water per formula weight. If the heating is stopped at 260°C, the weight loss rate becomes extremely low. Therefore, the composition of the sample remains virtually unchanged for some time, and it is practically the same as the starting material. Under these conditions, an X-ray powder diffraction analysis can be performed. On the other hand, if the heating is stopped before the above-mentioned phase transition is finished, the rate of water loss is high, and a fast dehydration of the sample is observed.

Note that our experimental data and previous literature data (7, 10, 11) seem to exclude the formation of partially dehydrated phases during heating. The thermal behavior of microcrystalline powders of α-ZrP as a function of heating

rate can be described by two limiting sequences of events. For heating rates equal to or lower than $\simeq 5°C/min$, the sequence is that of Figs. 1a and 2a; for heating rates higher than $\simeq 20°C/min$ the behavior is that shown in Figs. 1c and 2c. When heating rates between 5 and 20°C/min were used, an overlapping of the two above-mentioned reaction paths was observed.

X-ray Powder Diffraction Studies: Some Structural Considerations

The XRD patterns of samples of microcrystalline α-$ZrP \cdot H_2O$ heated at a rate of 50°C/min were taken at different temperatures.

As a consequence of the relatively high rate of dehydration, the pattern taken at 160°C was observed to change quickly over time, and it was impossible to obtain accurate data. However, a rapidly collected pattern taken at 170°C is reported in Fig. 7b. The pattern is markedly different from that taken at room temperature (Fig. 7a), the first peak being at $d = 7.50$ Å, showing that the following phase transition occurred:

$$\alpha\text{-}ZrP \cdot H_2O(7.56) \rightleftharpoons \alpha\text{-}ZrP \cdot H_2O(7.50).$$

A first attempt to index the pattern gave a monoclinic cell with the a and b parameters typical of α-phases, i.e., $a = 9.36$ Å, $b = 5.30$ Å, $c = 15.452$ Å, $\beta = 102.95°$.

The second phase transition was better studied. A more accurate X-ray powder pattern was collected at 250°C, and it is reported in Fig. 7c. The interlayer distance is 7.45 Å, so the process can be expressed as follows:

$$\alpha\text{-}ZrP \cdot H_2O(7.50) \rightleftharpoons \alpha\text{-}ZrP \cdot H_2O(7.45).$$

Note that the interlayer distances of the above phases are in fairly good agreement with those calculated on the basis of dilatometric experiments on large crystals (7.50 and 7.47 Å, respectively).

The pattern of the latter phase was well indexed by an hexagonal cell: $a = 5.366(4)$ Å, $c = 22.21(2)$ Å, $M(14) = 89$.

All the reflection indices satisfied the condition $-h + k + l = 3n$. Furthermore, the pattern exhibits a strong analogy with that of α-$ZrP \cdot 1/2H_2O$, heated over 70°C. The structure of the hemihydrate phase was recently solved by X-ray powder methods (17). The compound presented a phase transition at about 70°C, without water loss, which leads to a trigonal hemihydrate phase, space group $R\bar{3}$, having cell parameters $a = 5.3743$ Å, $c = 21.982$ Å, close to those found in the present study. The transition to the rhombohedral modification produces a sort of stabilization of the interlayer water, since water loss occurs at temperatures much higher than 100°C (17). This behavior is very similar to that observed for the monohydrate phase obtained at 250°C, which loses water at a very slow rate.

In conclusion we can assume that the structure of α-$ZrP \cdot H_2O$(7.45), which is generated after rapid heating to 250°C, is closely related to that of α-$ZrP \cdot 1/2H_2O$(7.30), present over 70°C.

Figure 8 shows the hypothetical structure of α-$ZrP \cdot H_2O$(7.45). For the sake of comparison, the structure of α-$ZrP \cdot H_2O$(7.56) at room temperature is also given. The transition at 250°C produces a slight changes in the atomic positions, which leads to a higher symmetry. The layers are shifted in relation to each other by $2/3a$ and $1/3b$, generating an ABC-type stacking and the P–OH groups are perpendicular to the layer plane, whereas they are slightly tilted in the room temperature phase. The water molecules are located at the center of the hexagonal zeolitic cage formed by six OH groups belonging to faced layers and lying almost on the same plane. These OH groups are about 3.25 Å apart and are slightly more interpenetrated than in the original phase. These modest structural changes may explain the stabilization of the hydration water after the phase transition.

Unfortunately the geometry and constructional peculiarity of the high-temperature X-ray camera cannot provide the accuracy required for more detailed structural studies.

A scheme of the reactions that summarizes previous and new results on the α-ZrP system, when heated at various temperatures, with different heating rates, is shown in Fig. 9. This scheme also takes into account previous studies of the hemihydrate phase.

Note that the sequence of events occurring during the heating of α-$ZrP \cdot H_2O$(7.56) may be described by two heating paths: a "high-rate" path, similar to that observed for large crystals, that involves the transitions of the monohydrate, and a "low-rate" path observed when microcrystalline powder is heated at rates equal to or lower than 5°C/min. Until now, it has not been possible to convert the monohydrate into the hemihydrate phase by thermal treatment.

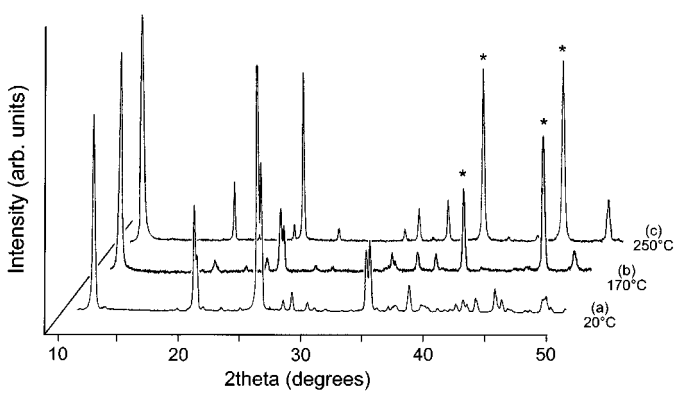

FIG. 7. XRD powder patterns of microcrystalline α-$ZrP \cdot H_2O$ taken at the indicated temperatures. Heating rate: 50°C/min. The peaks marked with an asterisk belong to the platinum sample-holder.

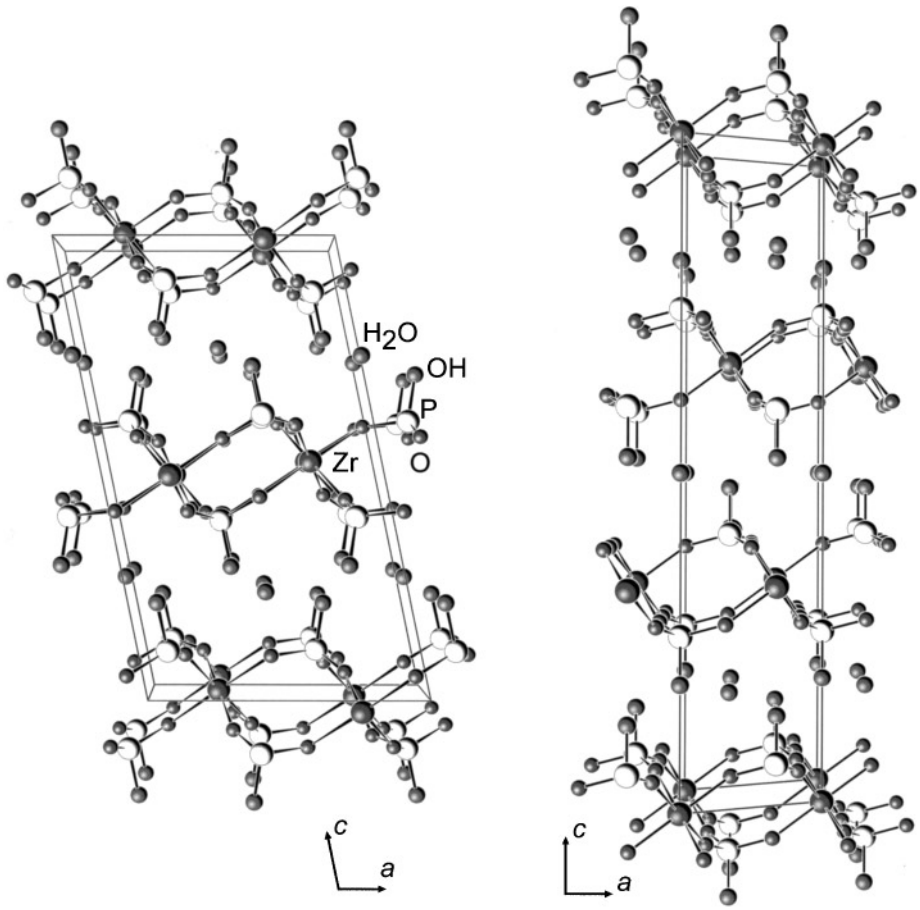

FIG. 8. Schematic structure of α-ZrP · H_2O(7.45) at 250°C (right), drawn on the basis of that of α-ZrP · 1/2H_2O(7.30) (17). The structure of α-ZrP · H_2O at room temperature, taken from ref. 5 is also reported for comparison (left).

CONCLUSION

By means of this and previous works, a deeper knowledge of this complex and fascinating system has been achieved. The structure of some of the phases shown in Fig. 9 have already been solved, while others are still being studied. More detailed structural investigation is therefore desirable to fully understand the crystallochemistry of the system.

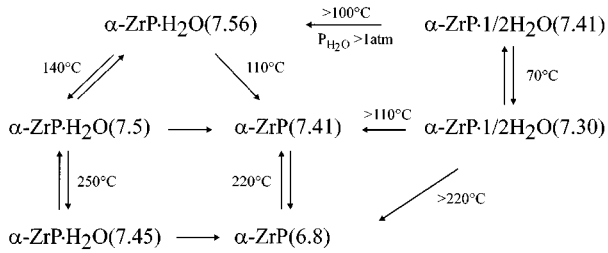

FIG. 9. Scheme of thermally induced phase transitions of hydrated and anhydrous phases of α-ZrP.

ACKNOWLEDGMENTS

Research was carried out in the Framework of the Agreement for Scientific Cooperation between the Italian C.N.R. and the Academy of Sciences of the Czech Republic.

REFERENCES

1. G. Alberti, M. Casciola, U. Costantino, and R. Vivani, *Adv. Mater.* **8,** 291 (1996).
2. A. Clearfield and U. Costantino, *in* "Two and Three-Dimensional Inorganic Networks" (G. Alberti and T. Bein, Eds.), Comprehensive Supramolecular Chemistry, Vol. VII, Chap. 4. Pergamon Press, Oxford, UK, 1996.
3. G. Alberti, *in* "Two and Three-Dimensional Inorganic Networks" (G. Alberti and T. Bein, Eds.), Comprehensive Supramolecular Chemistry, Vol. VII, Chap. 5. Pergamon Press, Oxford, UK, 1996.
4. A. Clearfield and G. D. Smith, *Inorg. Chem.* **8,** 431 (1969).
5. A. Clearfield and J. M. Troup, *Inorg. Chem.* **16,** 3311 (1977).
6. J. Albertsson, Å. Oskarsson, R. Teilgren, and J. O. Thomas, *J. Phys. Chem.* **81,** 1574 (1977).

7. A. Clearfield and S. Pack, *J. Inorg. Nucl. Chem.* **37,** 1283 (1975).
8. A. Clearfield, *in* "Inorganic Ion Exchange Materials" (A. Clearfield, Ed.), Chap. 1. CRC Press, Boca Raton, FI, 1982.
9. A. La Ginestra, M. A. Massucci, C. Ferragina, and N. Tomassini, *in* "Thermal Analysis — Proceedings, 4th ICTA, Budapest, 1974," Vol. 1, p. 631. Heyden, London, 1975.
10. A. La Ginestra, C. Ferragina, M. A. Massucci, P. Patrono R. Di Rocco, and A. G. Tomlinson, *Gazz. Chim. It.* **113,** 357 (1983).
11. D. Dollimore, N. J. Manning, and D. V. Nowell, *Thermochim. Acta* **19,** 37 (1977).
12. U. Costantino and A. La Ginestra, *Thermochim. Acta* **58,** 179 (1982).
13. G. Schuck, R. Melzer, R. Sonntag, R. E. Lechner, A. Bohn, K. Langer, and M. Casciola, *Solid State Ionics* **77,** 55 (1995).
14. G. Alberti, U. Costantino, and R. Giulietti, *J. Inorg. Nucl. Chem.* **42,** 1062 (1980).
15. G. Alberti and E. Torracca, *J. Inorg. Nucl. Chem.* **30,** 317 (1968).
16. P. E. Werner, L. Erikson, and M. Westerdahl, *J. Appl. Crystallogr.* **18,** 367 (1985).
17. G. Alberti, U. Costantino, R. Millini, G. Perego, and R. Vivani, *J. Solid State Chem.* **113,** 289 (1994).